Contribution from the Department of Chemistry and Materials Science Center,
Cornell University, Ithaca, New York 14853

Conjugation in the Three-Connected Net: The AlB₂ and ThSi₂ Structures and Their Transition-Metal Derivatives

Chong Zheng[†] and Roald Hoffmann*

The local environment in a hexagonal net (graphite, AlB₂) and the ThSi₂ structure resembles planar or rotated conformations of trimethylenemethane, C(CH₂)₃. This electronic relationship is traced into the band structure of the extended materials. When the π* band in either the discrete molecule or the nets of Si is more than half-filled (more than 4 electrons per Si), there is a driving force favoring the less conjugated rotated geometries. An analysis is given of the more complicated rotation in the SrSi₂ structure and of the electronic structure of transition-metal derivatives of these nets, especially LaPtSi.

Three-connected nets occur often in extended structures. They may be planar, as in the layers of graphite, **1**,[1] or puckered, as
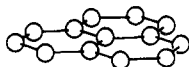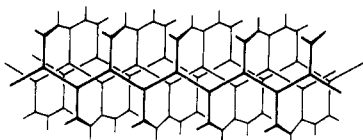

1

in the the elemental α-arsenic structure **2**.[2] More complicated
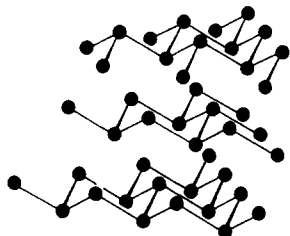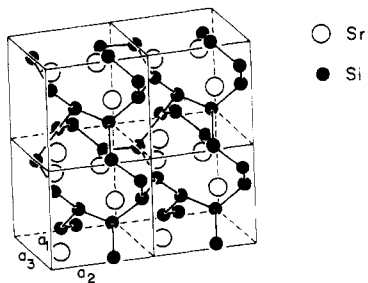

2

geometrical arrangements abound. For instance in the ThSi₂ structure **3**, the Si sublattice forms a three-connected net, trigonal

3

at each Si, but different from graphite.[3] In SrSi₂,[4] **4**, a still

4

different net is chosen, one that is slightly pyramidal at each Si. Various ternary transition-metal compounds, exemplified by GdCuSi,[5] LaIrSi,[6] and LaPtSi,[7] crystallize in one or another of

Table I. Some Late-Transition-Metal Ternary ABC Compounds

compound	structure type[a]	formal d electron count[b]	ref
SrZnGe	AlB₂	d¹⁰	14
RCuSi[c]	AlB₂	d⁹–d¹⁰	14, 24, 25
RCuGe[c]	AlB₂	d⁹–d¹⁰	14, 24, 25
MnFeGe	Ni₂In	"d⁶"	26
MnCoGe	Ni₂In	"d⁷"	27
MnNiGe	Ni₂In	"d⁸"	28
CaCuSb	Ni₂In	d¹⁰	29
SrCuSb	Ni₂In	d¹⁰	29
CaCuBi	Ni₂In	d¹⁰	29
SrCuBi	Ni₂In	d¹⁰	29
CaCuGe	distorted AlB₂	d⁹	23
RPdSb[d]	CaIn₂	d⁹–d¹⁰	31
RCuSn[d]	CaIn₂	d⁹–d¹⁰	25
RAuSn[d]	CaIn₂	d⁹–d¹⁰	25
RPtSi[e]	LaPtSi (ordered ThSi₂)	d⁹	7
LaIrSi	LaIrSi (ordered SrSi₂)	d⁸	6
RPtSi[f]	LaIrSi	d⁸	30

[a] Ni₂In and AlB₂ are class-equivalent but not lattice-equivalent since $c(Ni_2In) = 2c(AlB_2)$. CaIn₂ is puckered AlB₂ type. [b] Assuming Mn²⁺ in MnFeGe, MnCoGe, and MnNiGe. [c] R = Ca, Sr, Bu, Y, La, Ce, Pr, Nd, Sm, Gd, Tb, Dy, Ho, Er, Tm, Lu. [d] R = rare-earth metal. [e] R = La, Ce, Dr, Nd, Sm, Gd. [f] R = Ca, Eu, Sr, Ba.

these structural types. These then incorporate a transition metal and a main-group element into the structure.

Nor is the variety of trigonal nets exhausted by these. Many others occur in extended structures.[8]

One would like to understand the similarities and differences between these various three-connected structures, and how different compounds decide for one type and not another.

There is also an interesting connection to be made to a discrete organic molecule. This is trimethylenemethane, **5**, a kinetically

(1) Donohue, J. *The Structures of the Elements* Robert E. Krieger Publishing Co.: Malabar, FL, 1982; p 258.
(2) Reference 1; p 3 ,2.
(3) (a) Brauer, G.; Mitius, A. *Z. Anorg. Chem.* **1942**, *249*, 325. A similar structure has been suggested for a hypothetical metallic carbon allotrope. (b) Hoffmann, R.; Hughbanks, T.; Kertesz, M.; Bird, P. H. *J. Am. Chem. Soc.* **1982**, *105*, 4831.
(4) (a) Janzon, K.; Schäfer, H.; Weiss, A. *Angew. Chem.* **1965**, *77*, 258. (b) Pringle, G. E. *Acta Crystallogr., Sect. B* **1972**, *28*, 2326.
(5) Parthé, E. *Colloq. Int. C.N.R.S.* **1970**, *180*, 61.
(6) Klepp, K.; Parthé, E. *Acta Crystallogr., Sect. B* **1982**, *38*, 1541.
(7) Klepp, K.; Parthé, E. *Acta Crystallogr., Sect. B* **1982**, *38*, 1105.
(8) See, for example: (a) Wells, A. F. *J. Solid State Chem.* **1984**, *54*, 378. (b) Wells, A. F. *Three-Dimensional Nets and Polyhedra* Wiley: New York, 1977. Burdett and co-workers have analyzed various three-connected nets such as CaB₂C₂, black phosphorus, and arsenic structures: (c) Burdett, J. K. *Struct. Bonding (Berlin)* **1987**, *65*, 29; *Prog. Solid State Chem.* **1984**, *15*, 173; *Adv. Chem. Phys.* **1982**, *49*, 47. (d) Burdett, J. K.; Canadell, E.; Hughbanks, T. *J. Am. Chem. Soc.* **1986**, *108*, 3971. (e) Burdett, J. K.; Lee, S. *J. Am. Chem. Soc.* **1985**, *107*, 3063; **1983**, *105*, 1079. (f) Burdett, J. K.; Lin, J. H. *Acta Crystallogr., Sect. B* **1982**, *38*, 408.

[†]Present address: Department of Chemistry, University of Houston, Houston, Texas 77004
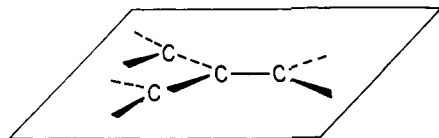
5

unstable but detectable[9] organic species that has for a long time served as a focus of experimental synthetic effort and theoretical discussion.[10]

The geometrical discussion around trimethylenemethane has centered on the rotation of the methylene groups out of the carbon plane. Is the molecule all planar, as indicated in **5**; or, is one methylene group twisted 90° out of planarity, as in **6**? Do still
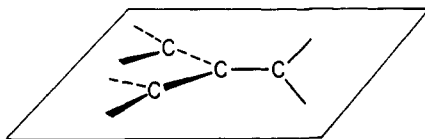
6

more complicated deformations occur? The problem is well analyzed;[10] as more π-electrons are added (after the four of the neutral carbon species), twisted, less conjugated structures are favored. There are important subtleties of electron count and spin state.[10]

It is obvious that there is a geometrical relationship between the graphite structure **1** and the all-planar trimethylenemethane building block **5**. The ThSi$_2$ structure **3** contains the singly rotated element **6**. Can deeper connections be drawn?

This paper addresses these questions, with molecular and band calculations of the extended Hückel type. The computational details are in the Appendix. To compare various structures we focus on two representative elements—Si for the main-group element structures and Pt and Si for the transition-metal analogues. All specific calculations in this paper refer to these elements.

General Considerations

In all three-connected nets that are under consideration here each vertex forms three σ bonds. Furthermore, there is at least one π bond; i.e., the local trimethylenemethane-like geometry allows good π overlap between a given E atom and at least one neighbor (actually three such overlaps in **5** and two in **6**). And

there are four or more electrons per E atom in the net.

We can then follow a schematic evolution of the electronic structure of these nets. Imagine sp^2 hybridization at each center, as on the left side of **7**. Next double the levels, taking two atoms
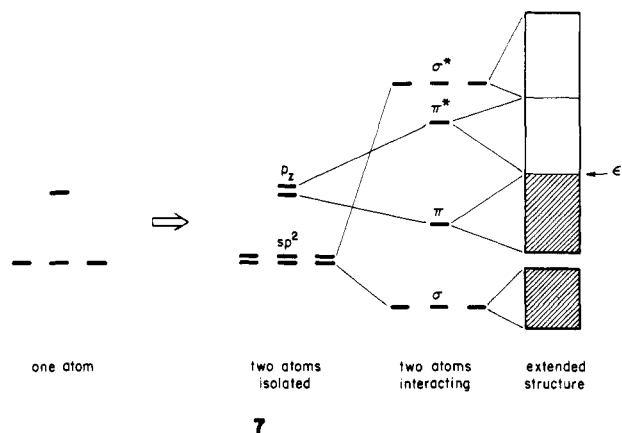

7

per unit cell (as there actually are in the graphite net). Then turn on the σ and π interactions—three σ levels go down; three σ^* levels go up. π and π^* levels, split by less, are formed. Each of these levels develops into a band when extended interaction are turned on. For atoms with four valence electrons, the π band is completely filled. Thus, one would expect structures that allow maximum π overlap (stabilizing π and destabilizing π^*) would be favored. When more electrons are added to the system, one might anticipate the reverse. Let us see how this general, schematic picture holds up in the detailed analysis.

The Graphite Structure

The hexagonal net allows maximal π overlap. Its band structure is well-known.[11a] Figure 1a shows the calculated band structure for Si. The π bandwidth is 9.97 eV. The important degeneracy of π and π^* at the K point can be understood in the following way:[11b] the two z orbitals in the unit cell form bonding and antibonding combinations. As a consequence of Bloch's theorem,[12] neighboring cells are combined in the wave function with a phase factor $e^{i\phi}$ or $e^{-i\phi}$ (see **8**, **9**) at the K point $(^1/_3, ^2/_3)$, $\phi = 2\pi/3$.
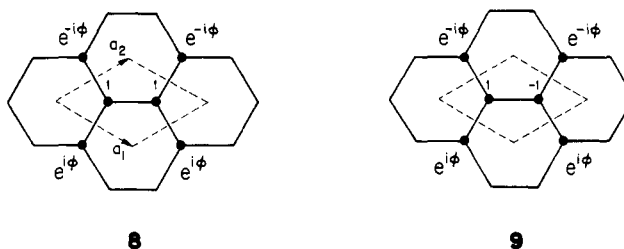
8　　　　　　　　　　**9**

The bond order inside the unit cell for the bonding combination **8** (coefficients 1 and 1) is 1. Each of the four inter-cell bonds contributes -0.5 (1 and $e^{i\phi}$). The total bond order is -1. The antibonding combination **9** also has a bond order of -1. The analysis can be extended to next-nearest-neighbor interactions and so on. Hence π and π^* are degenerate at K, giving rise to the characteristic semimetallic nature of graphite.

When the two atoms in the unit cell are different, as in the case of BN, the bond order for the bonding (1 and δ) and antibonding combinations (δ and -1) will be different. A gap at K should be opened up, resulting in a semiconductor or an insulator. This is similar to Y-aromatic molecular systems where heteroatomic substitutions split the nonbonding degenerate levels and thus stabilize the molecules.[11c-e]

(9) (a) Dowd, P.; Sachdev, K. *J. Am. Chem. Soc.* **1967**, *89*, 715. (b) Dowd, P. *Acc. Chem. Res.* **1972**, *5*, 242. (c) Dowd, P.; Chow, M. *J. Am. Chem. Soc.* **1977**, *99*, 2825, 6438; *Tetrahedron* **1982**, *38*, 799.

(10) (a) Skell, P. S.; Doerr, R. S. *J. Am. Chem. Soc.* **1967**, *89*, 4688. (b) Doerr, R. G.; Skell, P. S. *J. Am. Chem. Soc.* **1967**, *89*, 3062. (c) Borden, W. T. *Tetrahedron Lett.* **1967**, *3*, 259; *J. Am. Chem. Soc.* **1975**, *97*, 2906; **1976**, *98*, 2695. (d) Gold, A. *J. Am. Chem. Soc.* **1964**, *91*, 4961. (e) Dewar, M. J. S.; Wasson, J. S. *J. Am. Chem. Soc.* **1971**, *93*, 3081. (f) Yarkony, D. R.; Schaefer, H. F., III. *Chem. Phys. Lett.* **1975**, *35*, 291. (g) Davis, J. H.; Goddard, W. A., III. *J. Am. Chem. Soc.* **1976**, *98*, 303; **1977**, *99*, 4242. (h) Davidson, E. R.; Borden, W. T. *J. Chem. Phys.* **1976**, *64*, 663. (i) Baseman, R. J.; Pratt, D. W.; Chow, M.; Dowd, P. *J. Am. Chem. Soc.* **1976**, *98*, 5726. (j) Platz, M. S.; Berson, J. A. *J. Am. Chem. Soc.* **1976**, *98*, 6743. (k) Hood, D. M.; Pitzer, R. M.; Schaefer, H. F., III. *J. Am. Chem. Soc.* **1978**, *100*, 2227. (l) Schoeller, W. W. *J. Chem. Soc., Perkin Trans.* **1978**, *2*, 525. (m) Worley, S. D.; Webb, T. R.; Gibson, D. H.; Ong, T. S. *J. Organomet. Chem.* **1979**, *168*, C16. (n) Schoeller, W. W.; Yurtsever, E.; Shillady, D. D. *Nouv. J. Chim.* **1979**, *3*, 603. (o) Claesson, O.; Lund, A.; Gillbro, T.; Ichikawa, T.; Edlund, O.; Yoshida, H. *J. Chem. Phys.* **1980**, *72*, 1463. (p) Feller, D.; Borden, W. T.; Davidson, E. R. *J. Chem. Phys.* **1981**, *74*, 2256. (q) Auster, S. B.; Pitzer, R. M.; Platz, M. S. *J. Am. Chem. Soc.* **1982**, *104*, 3812. (r) Borden, W. T.; Davidson, E. R.; Feller, D. *Tetrahedron* **1982**, *38*, 737. (s) Said, M.; Maynau, D.; Malrieu, J. P.; Garcia-Bach, M. A. *J. Am. Chem. Soc.* **1984**, *106*, 571. (t) Feller, D.; Davidson, E. R.; Borden, W. T. *Isr. J. Chem.* **1983**, *23*, 105. (u) Wilhelm, D.; Dietrich, H.; Clark, T.; Mahdi, W.; Kos, A. J.; Schleyer, Paul v. R. *J. Am. Chem. Soc.* **1984**, *106*, 7279. (v) Rajca, A.; Rice, J. E.; Streitwieser, A., Jr.; Schaefer, H. F., III. *J. Am. Chem. Soc.* **1987**, *109*, 4189.

(11) (a) Wallace, P. R. *Phys. Rev.* **1947**, *71*, 622. (b) Kertesz, M.; Hoffmann, R. *J. Am. Chem. Soc.* **1984**, *106*, 3453. (c) Hoffmann, R. *J. Am. Chem. Soc.* **1968**, *90*, 1475. (d) Gleiter, R.; Hoffmann, R. *Angew. Chem., Int. Ed. Engl.* **1969**, *8*, 214. (e) Gund, P. *J. Chem. Educ.* **1972**, *49*, 100.

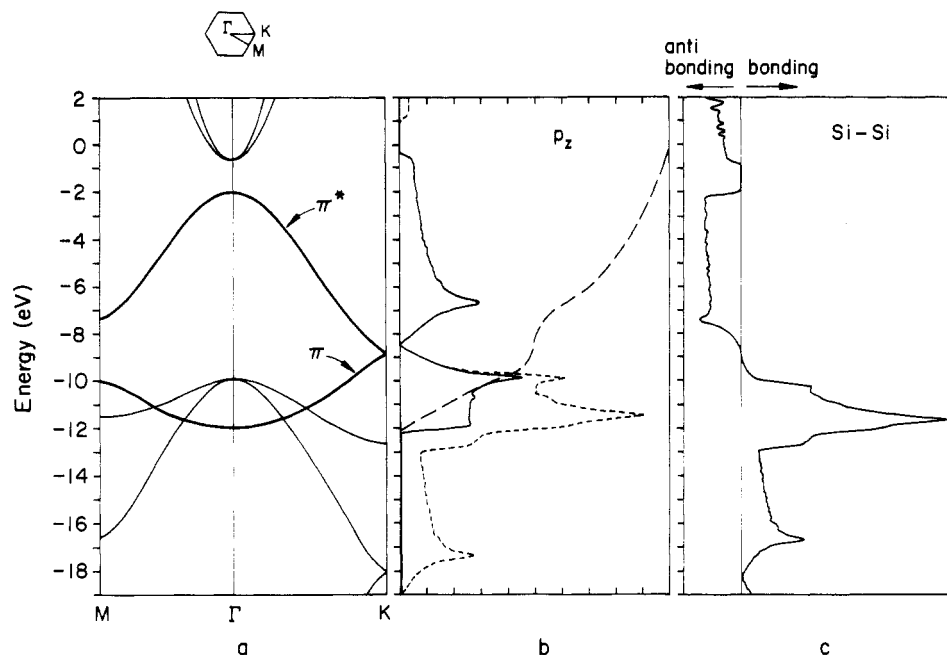(12) Ashcroft, N. W.; Mermin, N. D. *Solid State Physics*; Saunders: Philadelphia, PA, 1976; p 133.

Figure 1. (a) Band structure of a graphite type Si sheet. (b) Density of states (DOS): dotted line, total DOS; solid line, contribution from p_z (orbital perpendicular to the sheet); dashed line, integration of p_z DOS. (c) Crystal overlap population (COOP) curve for the Si–Si bond.
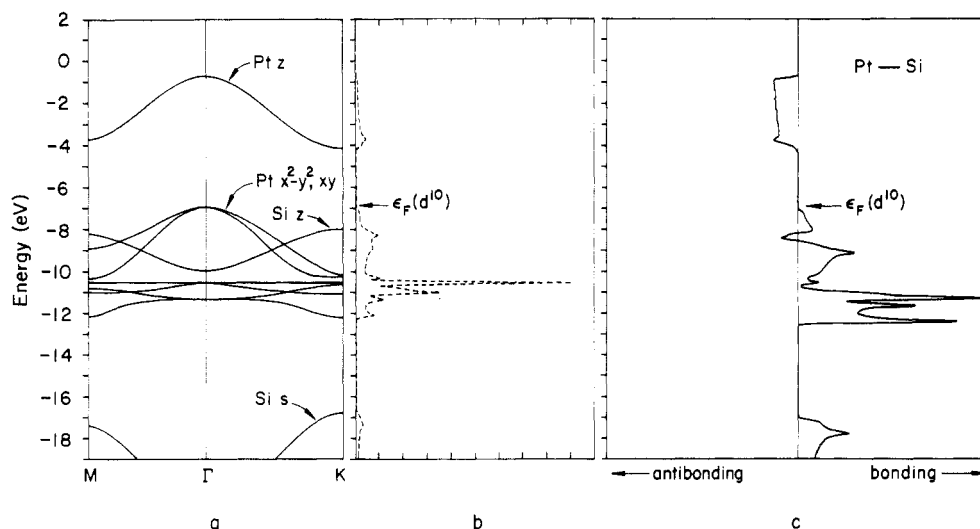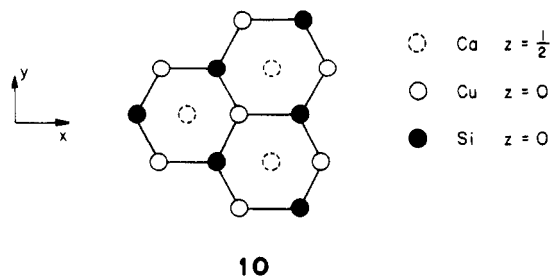

Figure 2. (a) Band structure of an AlB_2 type PtSi sheet. (b) Total density of states. The flat band and thus the peak in this DOS at -10.5 eV is mostly d_{z^2}. (c) COOP curve for the Pt–Si bond in the AlB_2 type PtSi structure.

Many transition-metal compounds use the simple hexagonal net as a building block. The important parent structure here is the AlB_2 structure. There are many late-transition-metal compounds,[13] with formal d^9 or d^{10} electron counts, which crystallize in this form. Examples are $CaCuSi$[14] (**10**) and $SrZnGe$.[14]

10

What would one expect in a band structure of an EM hexagonal net, such as that calculated for E = Si, M = Pt in Figure 2? One can still form sp^2 hybrids on Pt, and though these will be much higher in energy than the corresponding Si hybrids, they will interact pretty well. But now there are d orbitals on Pt. A local crystal field argument (assuming "ligand" (Si) donor functions below metal d functions, more on this below) will readily order this in energy. The $x^2 - y^2$, xy combination should be highest and xz, yz next, with z^2 least affected by the neighbor silicons.

This is in fact what happens, though there are interesting small complications. In Figure 2 at the bottom is the Si 3s band, followed by the Si p and Pt d bands. The Pt z^2 band is very narrow. The absence of degeneracy of the Pt and Si bands at K was anticipated from the previous discussion.

One special feature is the band that runs over the energy range -8 to -10 eV. It has substantial Si z character. One usually assumes that the "ligand" (Si) orbitals are below the metal ones. But in the case of Pt and Si (or Cu and O in the high T_c superconductors!) that may not be so. In fact our parameters put Si z above Pt xz. So one should be aware of the possibility of

(13) The early-transition-metal compounds with a puckered AlB_2 structure and the planar AlB_2 transition-metal borides have been analyzed in detail: (a) Burdett, J. K.; Miller, G. J. *J. Am. Chem. Soc.* **1987**, *109*, 4092. (b) Burdett, J. K.; Canadell, E.; Miller, G. J. *J. Am. Chem. Soc.* **1986**, *108*, 6561.

(14) Rieger, W.; Parthé, E. *Monatsh. Chem.* **1969**, *100*, 439.
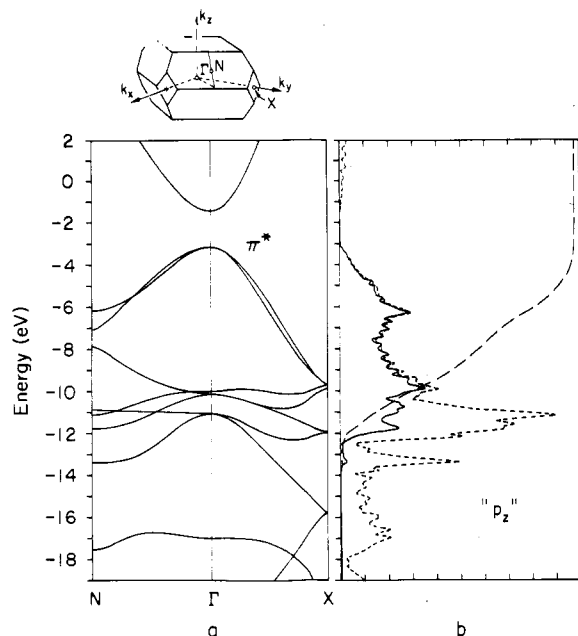
Figure 3. (a) Band structure of the 3-D $ThSi_2$ net. (b) DOS: dotted line, total contribution; solid line, contribution from p_z (p orbital perpendicular to the polyene plane); dashed line, integration of p_z DOS.

an inverse crystal field splitting.

Another interesting detail of the band structure, which would be seen if Figure 2 were shown at greater energy magnification, is that the flat band at -10.5 eV is really made up of two bands. One is Pt z^2. The other is a dδ band. The dδ band is a combination of xz and yz that has δ symmetry with respect to neighboring Si. Thus, its overlap with Si orbitals (Si z shown in **11**) is zero. The


combination varies in different parts of the Brillouin zone. But on the average that band is half xz and half yz. Its counter-part is dπ, **12**, used in conjugation.

Also shown in Figure 2 is the COOP curve,[15] which is the overlap-population-weighted DOS. It tells us how much the states in a given energy interval contribute to bonding or antibonding in a specified chemical bond. Due to the mixing of metal s and x, y with d orbitals, i.e. spd hybridization, the d band actually contributes to bonding. A compound with an electron count close to d^{10} should be stable. Adding more electrons should destabilize the structure.

The $ThSi_2$ Structure

The three-dimensional three-connected net of the Si sublattice of the $ThSi_2$ structure was shown in **3** and is redrawn in **13**. Each

13
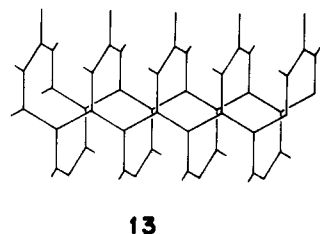
Si atom is in full conjugation with two neighbors, but its z orbital is perpendicular to the corresponding z orbital of the third
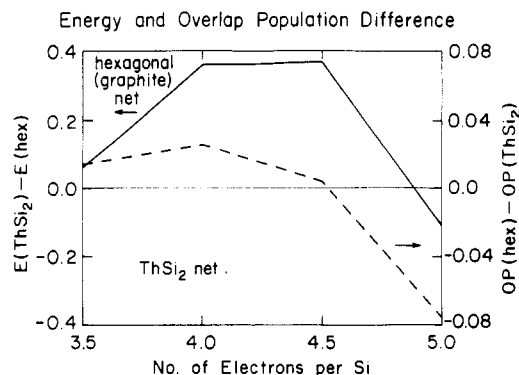
(15) Some other applications of the COOP curves may be found in the following references: (a) Wijeyesekera, S. D.; Hoffmann, R. *Organometallics* **1984**, *3*, 949. (b) Kertesz, M.; Hoffmann, R. *J. Am. Chem. Soc.* **1984**, *106*, 3453. (c) Saillard, J.-Y.; Hoffmann, R. *J. Am. Chem. Soc.* **1984**, *106*, 2006.

Figure 4. Energy per Si and overlap population difference between the 2-D hexagonal and 3-D $ThSi_2$ type structures. $E(ThSi_2) - E(hex) > 0$ means the hexagonal structure has the lower energy. Thus, the upper part is the hexagonal region and the lower part ($ThSi_2$ in lower energy) is the $ThSi_2$ region.

neighbor. The local bonding configuration is that of **6**. A new type of interaction comes into play in this relatively dense lattice, and this is a σ overlap between z orbitals of nonneighbor atoms of different chains, as indicated in **14**.

14
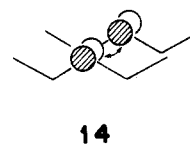
In a carbon net of type **3**, as studied by one of us earlier,[3b] if C–C is taken as 1.44 Å, the distance between polyene-type chains is 2.494 Å. Interaction **14** is strong. The π bandwidth for graphite and this structure are comparable. In a silicon net with Si–Si = 2.414 Å, the inter-chain distance is 4.181 Å. the inter-chain σ-type interaction drawn in **14** is weaker.

Figure 3 is the band structure of Si net **13**. There are four atoms per unit cell, so the number of bands is doubled (compared with Figure 1). Since **13** is a variant of **1**, many of the features of Figure 1 are retained. But there are differences. The most important one is that the bandwidth of the z band (the p orbital perpendicular to the polyene plane) is smaller. The top of the band (π^*, antibonding) is at -3 eV, compared to 0 eV in Figure 1. Thus, when π^* is heavily populated, the $ThSi_2$ net should be more favorable than the graphite type structure **1**. Figure 4 is the calculated energy and overlap population difference between the two structures. Indeed, as the π^* band is filled (more than 4.5 electrons per Si), the $ThSi_2$ structure should become more stable.

The $CaSi_2$ and $SrSi_2$ Nets

The $ThSi_2$ structure is not the only way to stabilize an electron-rich three-connected net structure. The π^* levels, be they in a hexagonal or $ThSi_2$ net, are antibonding between neighbors. Stabilization can be achieved by pyramidalizing at each carbon, locally creating a lone pair, as indicated in **15**. There are many
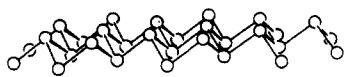

15

ways to fill space with puckered, pyramidal three-connected nets, and the structures of group 15 elements exhibit some of these.[16] So does the $CaSi_2$ structure,[17] whose Si net is shown in **16**. Under

(16) Particularly black phosphorus, α-arsenic, and α-antimony. See ref 1; Chapter 8.

high pressure, $CaSi_2$ transforms into the $ThSi_2$ structure type.[17d]

16

Still another way to limit conjugation, a necessity for electron-rich systems, is taught us by the $SrSi_2$ structure, **4**.[18] In this material, not only is the trimethylenemethane motif slightly puckered at each Si, but also each Si_3 group is turned 79.7° from another. The local arrangement is indicated in **17**. This twist
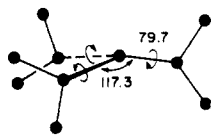

17

obviously also operates to reduce π antibonding in a net carrying formally 5 electrons/Si.

Figure 5a,b shows the total DOS and local z contribution for $CaSi_2$ and $SrSi_2$ nets. The top of the π^* band in $CaSi_2$ and in $SrSi_2$ is -4.7 and -5.8 eV, respectively, compared to 0 and -3 eV in the hexagonal and $ThSi_2$ structures (see Figures 1 and 3). The lowering of the π^* band top indicates even less π conjugation in geometries **16** and **17**. The calculated energy per Si atom in $CaSi_2$ and $SrSi_2$ structures is lower than that of the hexagonal structure by 0.13 and 0.66 eV, respectively, when the π^* band is singly occupied (5 electrons per Si).

It is the twist, not the slight pyramidalization in the $SrSi_2$ net (see **17**), that breaks the conjugation. A $SrSi_2$ type structure (space group $P4_332$) with a locally planar Si_3 motif is possible, with the crystal parameter $x = 0.375$ ($x = 0.428$ for $SrSi_2$). The structure, shown in **18**, is composed of parallel helices connected
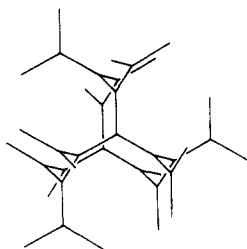
18

by trimethylenemethane-like moieties. Its DOS and contribution of local z states are shown in Figure 5c.

The π^* band dispersion is very similar to that of $SrSi_2$ in Figure 5b. The total energy of **18** per Si atom is slightly lower than that of $SrSi_2$ by 0.13 eV. But this is the consequence of a larger unit cell ($a = 6.83$ Å vs $a = 6.54$ Å for $SrSi_2$) and thus less dispersion of the π^* band from second neighbors, assuming equal Si-Si distances of 2.41 Å in both structures.

As in the Y-aromatic molecular case,[11c-e] the substitution of the nearest neighbors by heteroatoms can also limit conjugation. It is interesting to note that a substituted trimethylenemethane derivative with 6 π electrons, namely dilithium tribenzylidene-methane-2TMEDA, maintains a nearly planar structure.[10u]

Ternary Transition-Metal Derivatives

One transition metal analogue of $ThSi_2$ is the LaPtSi structure,
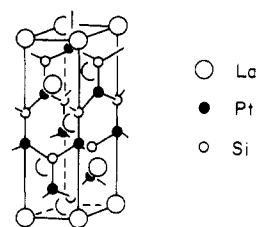
LaPtSi

19

because of their importance in semiconductor technology,[19] the ternary phases RM(Si,Ge) came to the fore only after the discovery of their superconductivity.[20]

The band structure and DOS of the PtSi sublattice of LaPtSi as shown in Figure 6. Since there are two PtSi units per cell, the number of bands is doubled (compared to Figure 2). As in the main-group case, many of the features are retained on going from an AlB_2 (graphite, BN) structure for PtSi to a $ThSi_2$ or LaPtSi structure. For example, z^2 is still a very narrow band. This is not surprising, since LaPtSi can be considered as a stacking variant of the AlB_2 type.[21] However, there are some differences. An important one, relevant to energetics, is the position of the Fermi level for d^{10} configuration ϵ_F (d^{10}). ϵ_F is now at -6.5 eV, compared to -7.0 eV for the hexagonal AlB_2 phase (see Figure 2). The orbital at the Fermi level is at the N point in the Brillouin zone. It has the composition illustrated in **20**.

20

The situation is reminiscent of discrete molecules such as $(PR_3)_2Ni$-ethylene. There orientations **21a** was favored over **21b**
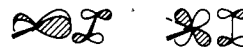

in plane   out of plane

a   b

21

because stabilizing interaction **22** is stronger than **23** for overlap

22   **23**

and energy gap reasons.[22] In the case of our extended structure, however, the counterpart of **22** is filled (or partially filled). Due to the 4-electron repulsion, arrangement **23** (corresponding to

(17) (a) Böhm, J.; Hassel, O. *Z. Anorg. Chem.* **1927**, *160*, 152. (b) Janzon, K. H.; Schäfer, H.; Weiss, A. *Z. Naturforsch., B* **1968**, *B23*, 1544. (c) Evers, J.; Oehlinger, G.; Weiss, A. *J. Solid State Chem.* **1977**, *20*, 173. (d) McWhan, D. B.; Compton, V. B.; Silverman, M. S.; Soulen, J. R. *J. Less-Common Met.* **1967**, *12*, 75.
(18) The angles are calculated from the crystal parameters of ref 4. The Si-Si-Si angle is different from that in ref 4a.

(19) (a) Sinha, A. K.; Marcus, R. B.; Sheng, T. T.; Haszko, S. E. *J. Appl. Phys.* **1972**, *43*, 3637. (b) Hosack, H. H. *J. Appl. Phys.* **1973**, *44*, 3476. (c) Anderson, R. M.; Reith, T. M. *J. Electrochem. Soc.* **1975**, *122*, 1338. (d) Bindell, J. B.; Colby, J. W.; Wonsidler, D. R.; Poate, J. M.; Conley, D. K.; Tisone, T. C. *Thin Solid Films* **1976**, *37*, 441. (e) Cohen, S. S.; Piacente, P. A.; Gildenblat, G.; Brown, D. M. *J. Appl. Phys.* **1982**, *53*, 8856. (f) Fontaine, C.; Okumura, T.; Tu, K. N. *J. Appl. Phys.* **1983**, *54*, 1404. (g) Herd, S.; Tu, K. N.; Ahn, K. Y. *Appl. Phys. Lett.* **1983**, *42*, 597. (h) Franciosi, A.; Weaver, J. H. *Phys. Rev. B* **1983**, *27*, 3554.
(20) (a) Braun, H. F. *Phys. Lett. A* **1980**, *75*, 386. (b) Braun, H. F.; Segre, C. U. *Solid State Commun.* **1980**, *35*, 735. (c) Braun, H. F.; Segre, C. U. *Ternary Superconductors*; Shenoy, G. K., Dunlap, B. D., Fradin, F. Y., Eds.; Elsevier-North-Holland: Amsterdam, 1981; p 239–242.
(21) Parthé, E. *Colloq. Int. C.N.R.S.* **1967**, *157*, 195.
(22) (a) Rösch, N.; Hoffmann, R. *Inorg. Chem.* **1974**, *13*, 2656. (b) Albright, T. A.; Hoffmann, R.; Thibeault, J. C.; Thorn, D. L. *J. Am. Chem. Soc.* **1979**, *101*, 3801. (c) Albright, T. A.; Burdett, J. K.; Whangbo, M.-H. *Orbital Interactions in Chemistry*; John Wiley & Sons: New York, 1985; p 366.
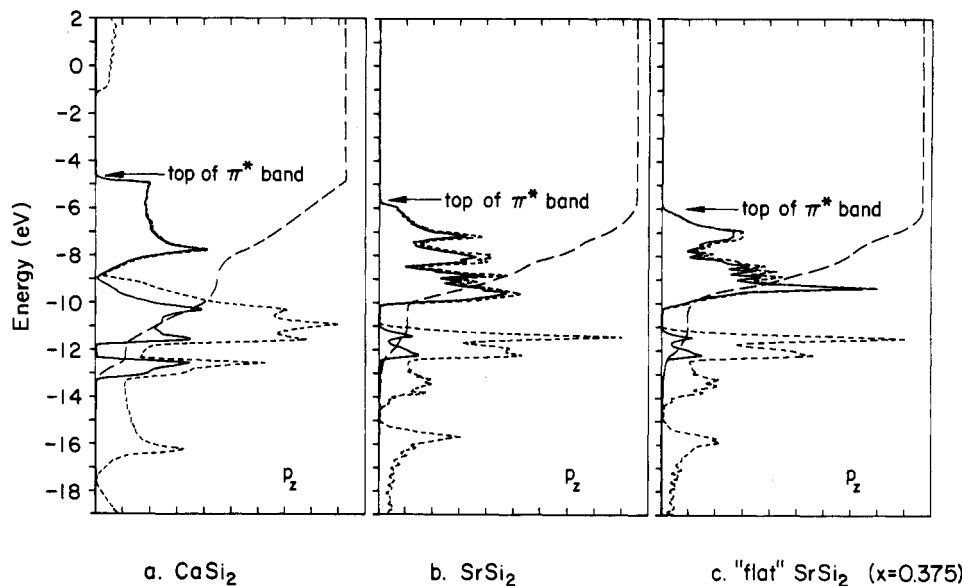
Figure 5. Total DOS of the $CaSi_2$ (a), the $SrSi_2$ (b), and the "flat" $SrSi_2$ with crystal parameter $x = 0.375$ (c) structures and the contribution to the DOS from the "p_z" states.
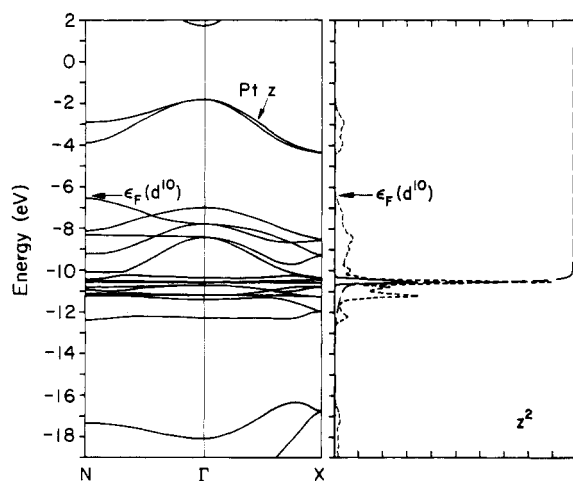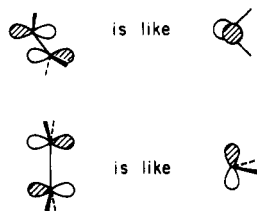

Figure 6. (a) Band structure of the 3-D LaPtSi net. (b) DOS: dotted line, total contribution; solid line, contribution from d_{z^2} (perpendicular to polyene-type chain plane); dashed line, integration of d_{z^2}.

AlB_2) should be more stable than **22** (LaPtSi). In making these arguments it is important to recall the reciprocal relationships of carbene and olefin ligands, indicated in **24**.

24

The calculated difference for d^{10} per formula is 0.5 eV, exactly the difference between the two $\epsilon_F(d^{10})$'s. For d^9, both AlB_2 and LaPtSi have the same energy. The DOS for LaIrSi structure, an ordered variant of $SrSi_2$, is shown in Figure 7. $\epsilon_F(d^{10})$ for LaIrSi is also −7.0 eV. The calculated energy of the LaIrSi net is higher than that for LaPtSi by 0.4 eV for d^{10} and 0.4 eV for d^9 and lower by 0.9 eV for d^8. In general the energetic difference between these structures should be small. Packing requirements may play a more important role in determining observed structures.

Finally we list some of the known ternary transition metal compounds of this type in Table I. As one can see, the structure is insensitive to electron count. A d^9 compound may adopt either LaPtSi or AlB_2 type geometries.
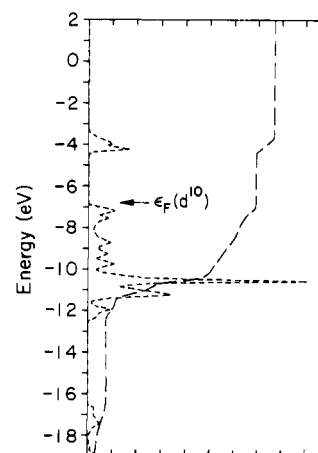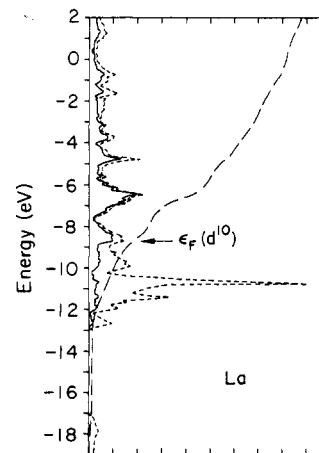

Figure 7. Total DOS of the LaIrSi type net.

Figure 8. Total DOS and the La contribution for the LaPtSi structure.

An interesting structural variant is provided by $CaCuGe$.[23] This is a distorted AlB_2 type material. One can think of it as

(23) Dörrscheidt, W.; Niess, N.; Schäfer, H. *Z. Naturforsch., B* **1977**, *32*, 985.

(24) Bodak, O. I.; Gladyshevskii, E. I.; Zarechnyuk, O. S.; Cherkashin, E. E. *Chem. Abstr.* **1967**, *66*, 89258y; *Wisnik Ser. Khim.* **1965**, *8*, 75.

(25) (a) Dwight, A. E. *Proceedings of the Seventh Rare Earth Research Conference*; NITS: Sringfield, VA, 1968. (b) Dwight, A. E. *Proceedings of the 12th Rare Earth Research Conference*; Denver Research Institute: Denver, CO, 1976; pp 480–489.

Table II. Extended Hückel Parameters

orbital	H_{ii}, eV	$\zeta_1{}^a$	ζ_2	$c_1{}^a$	c_2
Si 3s	−17.3	1.38			
3p	−9.2	1.38			
Pt 6s	−8.98	2.55			
6p	−4.18	2.53			
5d	−10.57	6.01	2.696	0.6333	0.5512
La 6s	−7.67	2.14			
6p	−5.01	2.08			
5d	−8.21	3.78	1.381	0.7765	0.4586

^{a} Exponents and coefficients in a double-ζ expansion of the 5d orbital.

$Ca^{2+}(CuGe)^{2-}$. Neglecting the cation and filled d core, one may consider it equivalent to $(GeGe')^+$. There would be a hole in the π band, which would provide a driving force to form bonds between layers. The observed structure is shown in **25**.
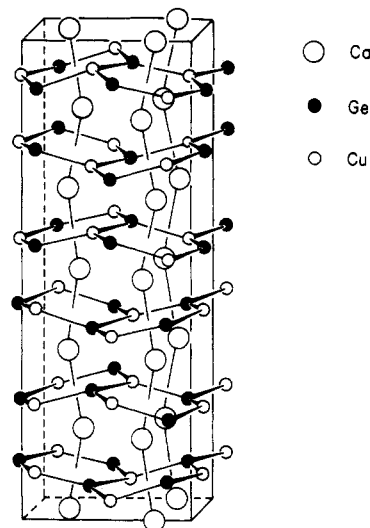
Finally, we show the DOS to LaPtSi calculated by including the cation La in Figure 8. Since La is more than 3.2 Å away from both Pt and Si, there is not much interaction between them. Figure 8 is essentially the DOS of PtSi net plus that of La. The DOS of PtSi is not changed much (cf. Figure 6). But around the Fermi level, there is a lot of contribution from La states. Thus, the presence of the cation will strongly affect the conducting and magnetic properties of the compound.

Appendix

The extended Hückel method[32] was used in the calculations.

CaCuGe

25

Since the extended Hückel total energy may not be reliable in situations where the distance is varied, we kept the Si–Si distance fixed at 2.414 Å (the distance in SrSi$_2$) and Si–Pt at 2.44 Å (ideal bond length in LaPtSi). Pt parameters were derived from charge iteration of LaPtSi, with 6 k points. 494 k points were used for the graphite and CaSi$_2$ structures, 396 for ThSi$_2$, 84 for SrSi$_2$, 494 for transition metal AlB$_2$ structure, 270 for LaPtSi, and 35 for LaIrSi. These are mesh points in the irreducible wedge of the Brillouin zone and were generated according to Pack and Monkhorst's method.[33] The extended Hückel parameters are listed in Table II.

(26) Suzuoka, T.; Adelson, E.; Austin, A. E. *Acta Crystallogr. A* **1968,** *24,* 513.
(27) Jeitschko, W. *Acta Crystallogr. B* **1975,** *31,* 1187.
(28) Castelliz, L. *Monatsh. Chem.* **1953,** *84,* 765.
(29) Eisenmann, B.; Cordier, G.; Schäfer, H. *Z. Naturforsch., B* **1974,** *29,* 457.
(30) Evers, J.; Oehlinger, G. *J. Solid State Chem.* **1986,** *62,* 133.
(31) Marazza, R.; Rossi, D.; Ferro, R. *J. Less-Common Met.* **1980,** *75,* P25.

(32) (a) Hoffmann, R. *J. Chem. Phys.* **1963,** *39,* 1397. Hoffmann, R.; Lipscomb, W. N. *J. Chem. Phys.* **1962,** *36,* 2179; **1962,** *37,* 2872. Ammeter, J. H.; Bürgi, H.-B.; Thibeault, J. C.; Hoffmann, R. *J. Am. Chem. Soc.* **1978,** *100,* 3686. (b) Whangbo, M.-H.; Hoffmann, R.; Woodward, R. B. *Proc. R. Soc. London* **1979,** *A366,* 23.
(33) Pack, J. D.; Monkhorst, H. *Phys. Rev. B* **1977,** *16,* 1748.

Electrocatalytic Activity of Electropolymerized Films of Bis(vinylterpyridine)cobalt(2+) for the Reduction of Carbon Dioxide and Oxygen

H. C. Hurrell,[†] A.-L. Mogstad,[†] D. A. Usifer,[‡] K. T. Potts,[‡] and H. D. Abruña*,[†]

Electropolymerized films of $[Co(v\text{-tpy})_2]^{2+}$ (v-tpy = 4′-vinyl-2,2′:6′,2″-terpyridine) are active catalytically in the electroreduction of both carbon dioxide and oxygen. The polymer films lower the overpotential of carbon dioxide reduction in DMF by nearly 1.0 V and the four-electron reduction of oxygen in aqueous solution by 300 mV. The predominant product of carbon dioxide reduction is formic acid, as determined by the chromotropic acid test. The product distribution (water vs peroxide) in the reduction of oxygen was strongly dependent on the polymer coverage, with water being the predominant product at high coverage ($>2.5 \times 10^{-9}$ mol/cm^2), whereas at lower coverage, hydrogen peroxide was the main reaction product.

Introduction

The reduction of carbon dioxide to useful fuel products and the four-electron reduction of oxygen to water at potentials close to those dictated by thermodynamics have attracted considerable interest in recent years.[1] These are particularly difficult reactions to catalyze because they involve multiple electron transfers that

are often coupled with other chemical steps, e.g. protonation, and in addition there can be other reaction pathways such as the

† Cornell University.
‡ Rensselaer Polytechnic Institute.

(1) (a) Fisher, B.; Eisenberg, R. *J. Am. Chem. Soc.* **1980,** *102,* 7361. (b) Lieber, C. M.; Lewis, N. S. *J. Am. Chem. Soc.* **1984,** *106,* 5033. (c) Webley, W. S.; Durand, R. R.; Anson, F. C. *J. Electroanal. Chem. Interfacial Electrochem.* **1987,** *229,* 273. (d) Holdcroft, S.; Funt, B. L. *J. Electroanal. Chem. Interfacial Electrochem.* **1987,** *225,* 177. (e) Collin, J.-P.; Jouaiti, A.; Sauvage, J.-P. *Inorg. Chem.* **1988,** *27,* 1986. (f) Cabrera, C. R.; Abruña *J. Electroanal. Chem. Interfacial Electrochem.* **1986,** *209,* 101.